LASER INTERFEROMETER GRAVITATIONAL WAVE OBSERVATORY

LIGO Laboratory / LIGO Scientific Collaboration

LIGO-T0900640-v2 *LIGO* February 2, 2010

Acceleration of the FFT simulation of stable cavity

Hiro Yamamoto

Distribution of this document:
LIGO Science Collaboration

This is an internal working note
of the LIGO Project.

California Institute of Technology
LIGO Project – MS 18-34
1200 E. California Blvd.
Pasadena, CA 91125
Phone (626) 395-2129
Fax (626) 304-9834
E-mail: info@ligo.caltech.edu

Massachusetts Institute of Technology
LIGO Project – NW17-161
175 Albany St
Cambridge, MA 02139
Phone (617) 253-4824
Fax (617) 253-7014
E-mail: info@ligo.mit.edu

LIGO Hanford Observatory
P.O. Box 1970
Mail Stop S9-02
Richland WA 99352
Phone 509-372-8106
Fax 509-372-8137

LIGO Livingston Observatory
P.O. Box 940
Livingston, LA 70754
Phone 225-686-3100
Fax 225-686-7189

http://www.ligo.caltech.edu/

1. Introduction

Second generation gravitational wave detectors using laser interferometry adopt a stable cavity configuration in the recycling cavity [1]. One realization is to place a mode matching telescope in the recycling cavity and makes the gouy phase of the recycling cavity large enough to suppress the degeneracy.

The field is focused to make the Rayleigh range small so that enough gouy phase is aquired through propagation in a limited length cavity. In the focusing cavity (FC) where mode parameter changes, the field curvature is small and the field exhibits very rapid oscillation in the plane perpendicular to the propagation direction. This makes it difficult to use a FFT-based simulation to calculate the field propagation through the cavity because the number of grid points needs to be large so that the initial boundary condition with rapid oscillation can be properly sampled.

An algorithm based on the adaptive grid size formulation of the FFT-based cavity simulation is shown to accelerate the calculation of fields propagating through a stable cavity adapted in the recycling cavity. This method allows the number of the grid points of the FFT calculation to be smaller than that needed when this algorithm is not used, and the simulation time can be reduced by an order of magnitude.

2. Focusing cavity (FC)

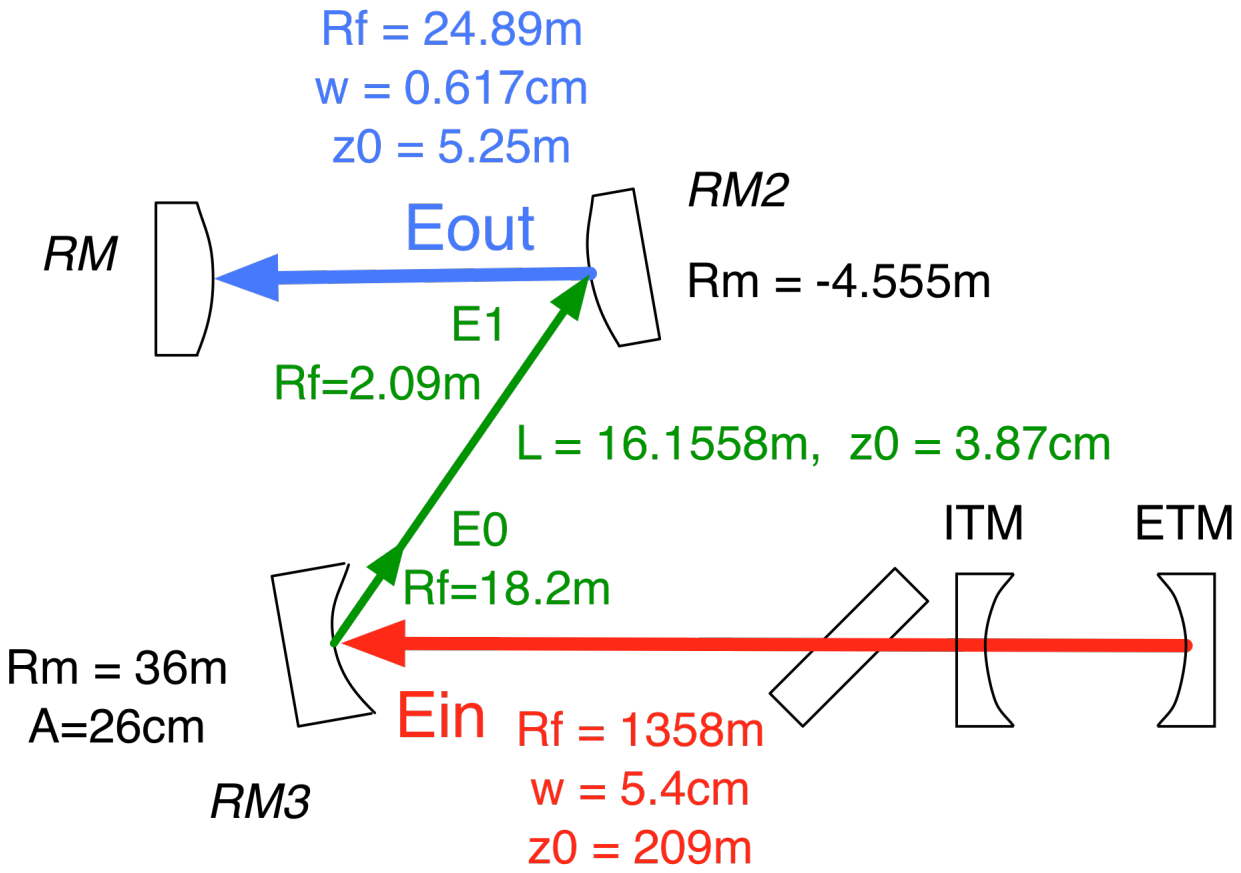

Figure 1 Focusing cavity (parameters from [2])

Figure 1 shows the advanced LIGO power recycling cavity [2] consisted of a recycling mirror, RM, a FC made of RM2 (ROC=-4.555m) and RM3 (ROC=36m), and ITM. Ein is the field going to RM3, and its field parameters are shown in red. Ein is reflected by RM3 to E0, and E0 propagates to RM2 to become E1. E1 is then reflected by RM2 to become Eout, and its parameters are shown in blue. The FC length is 16.1558m and the Rayleigh range in the cavity is very small, 3.87cm. The dominant part of the gouy phase comes from the cavity formed by RM and RM2, which accounts for 95% of the total gouy phase of the recycling cavity, 25°.

The ROC of E0 is 100 times smaller than that of Ein, and the ROC of E1 is 10 times smaller than that of Eout. E0 and Ein (E1 and Eout) have the same beam size on the reflecting mirror, so the spatial oscillation of E0 (E1) is much rapid than Ein (Eout). This causes the numerical simulation difficult as is discussed below.

In this document, the discussion is limited to the propagation from Ein to Eout in Figure 1, but the same argument applies to the reverse propagation.

The Fresnel approximation of the Huygen's integral propagating from z0 to z1 is given by the convolution of the source field at z_0, and the paraxial propagation kernel:

$$E(x_1,y_1,z_1) = \iint dx_0 dy_0 E(x_0,y_0,z_0)\cdot K(\Delta x,\Delta y,\Delta z)$$
$$\Delta x = x_1 - x_0,\ \Delta y = y_1 - y_0,\ \Delta z = z_1 - z_0 \qquad \textbf{(1)}$$

where K(x,y,z) is the paraxial propagation kernel defined as

$$K(x,y,z) = \frac{i}{z\cdot\lambda}\exp(-i\cdot k\cdot\frac{r^2}{2z}) \qquad (2)$$
$$r^2 = x^2 + y^2$$

When an incoming field, E_{in}, is reflected by a mirror with curvature R_m at normal incidence, the reflected field, E_0, acquires the following wave front phase:

$$E_0(x,y,z) = M_m(x,y,z)\cdot E_{in}(x,y,z)$$
$$= \overline{M_m}(x,y,z)\cdot\exp(i\cdot\phi(r))\cdot E_{in}(x,y,z) \qquad \textbf{(3)}$$
$$\phi(r) = k\cdot\frac{r^2}{R_m}$$

In this equation, M_m is the effect of the reflection by the mirror m, and $\overline{M}_m$ is the part after removing the phase by its curvature which is explicitly written as exp(iϕ). M_m is 0 outside of the mirror aperture. The field curvature changes by $-R_m/2$ by this reflection. The reflection map $\overline{M}_m$ contains effects of finiteness of the mirror aperture and surface aberration.

The field propagating from RM3 to RM2 is calculated by substituting the source field E_0 given by Eq. (3) in the propagation formula Eq. (1). The integration goes over the mirror RM3 surface.

When the field E_0 on RM3 is sampled with a spacing of dr, the phase change from r to r+dr is

$$d\phi = \frac{2k\cdot r\cdot dr}{R_m} \qquad \textbf{(4)}$$

In order to change the Rayleigh range in a short distance, curvature of the focusing mirror is small. With R_m=36m and r=5.4cm, the phase spacing in units of 2π is

$$\frac{d\phi}{2\pi} = \frac{2 \cdot 0.054}{36 \cdot 1.064 \times 10^{-6}} dr = 2800 \cdot dr \qquad (5)$$

The FFT-based simulation uses data values at grid points on the mirror surface. In order to have enough sampling points, e.g., 10, at this radius, the spacing should be $3.6\text{x}10^{-5}$m, or 9000 sampling points in a ±3 x beam size window. In the central region with smaller value of r, this number can be smaller, yet special care needs to be taken to use very large number of sampling points to properly handle this very rapid oscillation in the outer region.

3. Field propagation with magnification

When a field propagates from RM3 to RM2, the beam size becomes smaller by an order of magnitude. It was shown that a coordinate scaling is convenient to handle these cases [3, 4].

In order to magnify the beam size of E_1, the coordinate perpendicular to the propagation direction is scaled by a factor of α with the substitution of $x_1 = \alpha\, x_1'$ and $y_1 = \alpha\, y_1'$ in the propagation formula Eq. (1). With α < 1, the image size in the new coordinate system in (x_1', y_1') is magnified by 1/α.

By changing the arguments of the propagation kernel K from (x_1-x_0,y_1-y_0) to (x_1'-x_0,y_1'-y_0), the integral formula can be rewritten as follows:

$$\begin{aligned} E_1(x_1,y_1,z_1) &= \iint dx_0 dy_0 E_0(x_0,y_0,z_0)\cdot K(x_1-x_0,y_1-y_0,\Delta z) \\ &= \iint dx_0 dy_0 E_0(x_0,y_0,z_0)\cdot K(\alpha x_1'-x_0,\alpha y_1'-y_0,\Delta z) \\ &= \widetilde{C}(x_1,y_1,\Delta z,\alpha)\iint dx_0 dy_0 \widetilde{E}_0(x_0,y_0,z_0)\cdot K(x_1'-x_0,y_1'-y_0,\Delta z/\alpha) \end{aligned} \qquad (6)$$

where $\widetilde{E}$ and $\widetilde{C}$ are given as follows:

$$\begin{aligned} \widetilde{E_0}(x_0,y_0,z_0) &= \exp(i\cdot\phi_0(r_0))\cdot E_0(x_0,y_0,z_0) \\ \phi_0(r) &= k\cdot r^2\frac{(\alpha-1)}{2\Delta z} \end{aligned} \qquad (7)$$

$$\begin{aligned} \widetilde{C}(x_1,y_1,\Delta z,\alpha) &= \frac{1}{\alpha}\exp(i\cdot\widetilde{\psi}(r_1)) \\ \widetilde{\psi}(r) &= k\cdot r^2\frac{(1/\alpha-1)}{2\Delta z} = -\frac{1}{\alpha}\phi_0(r) = -\alpha\cdot\phi_0(r') \end{aligned} \qquad (8)$$

When E_0 is replaced by the expression using E_{in}, Eq. (3), $\widetilde{E}$ becomes as follows:

$$\tilde{E}_0(x_0,y_0,z_0) = \overline{M}_{m3}(x_0,y_0,z_0)\cdot\exp(i\cdot\phi_{in}(r_0))\cdot E_{in}(x_0,y_0,z_0)$$
$$\phi_{in}(r) = k\frac{r^2}{2\Delta z}\delta\alpha \qquad (9)$$
$$\alpha = \alpha_{opt} + \delta\alpha,\ \alpha_{opt} = 1 - \frac{2\Delta z}{R_{m3}}$$

where R_{m3} is the ROC of and M_{m3} is the reflection map of RM3.

If α is chosen to be

$$\alpha = \alpha_{opt} = 1 - \frac{2\Delta z}{R_{m3}} \qquad (10)$$

the rapidly oscillating phase in Eq. (3) is cancelled by the extra factor introduced by the coordinate scaling, ϕ_0 in Eq.(7). The oscillation can be suppressed when α is close to this optimal value or δα is small.

This optimal scaling factor α is a reasonable choice. The Rayleigh range in the FC is very small, and the beam size of a field is proportional to the distance to the waist position. The distance between RM3 and the waist position is $-R_{m3}/2$, and that of RM2 is $-R_{m3}/2 + \Delta z$ in this approximation, so the optimal value of α, Eq. (10), is approximately the ratio of the beam size on RM2 to that on RM3.

Field E_{out} is related to E_1 by the following equation, similar to Eq.(3):

$$E_{out}(x,y,z) = M_{m2}(x,y,z)\cdot E_1(x,y,z)$$
$$= \overline{M_{m2}}(x,y,z)\cdot\exp(i\cdot\phi(r))\cdot E_1(x,y,z) \qquad \mathbf{(11)}$$
$$\phi(r) = k\cdot\frac{r^2}{R_{m2}}$$

where R_{m2} is the ROC of and M_{m2} is the reflection map of RM2.

By combining this with Eq.(6), the field E_{out} is related to E_{in} by the following equation:

$$E_{out}(x_1,y_1,z_1) = C(x_1,y_1,\Delta z,\alpha)\iint dx_0 dy_0\,\tilde{E}_0(x_0,y_0,z_0)\cdot K(x_1'-x_0,y_1'-y_0,\Delta z/\alpha) \qquad (12)$$

where C is defined as follows:

$$C(x_1,y_1,\Delta z,\alpha) = \frac{1}{\alpha}\exp(i\cdot\psi(r_1))\cdot\overline{M}_{m2}(x_1,y_1,z_1)$$
$$\psi(r) = k\cdot r^2\left(\frac{1/\alpha-1}{2\Delta z} + \frac{1}{R_{m2}}\right) \qquad (13)$$
$$= -\frac{k}{2}r^2\left[\frac{\alpha_{opt}}{\alpha}\left(\frac{1}{-R_{m3}/2+\Delta z} - \frac{1}{R_{m2}/2}\right) - \frac{\delta\alpha}{\alpha}\left(\frac{1}{\Delta z} + \frac{1}{R_{m2}/2}\right)\right)$$

If you use the optimal value of α, Eq.(10), then this relation becomes simplified as follows:

$$E_{out}(x_1,y_1,z_1) = C(x_1,y_1,\Delta z,\alpha)\iint dx_0 dy_0 E_{in}(x_0,y_0,z_0)\cdot \overline{M}_{m3}(x_0,y_0,z_0)\cdot K(x_1'-x_0,y_1'-y_0,\Delta z/\alpha) \quad (14)$$

$$C(x_1,y_1,\Delta z,\alpha) = \frac{1}{\alpha}\exp(i\cdot\psi_{opt}(r_1))\cdot\overline{M}_{m2}(x_1,y_1,z_1)$$
$$\psi_{opt}(r) = -\frac{k}{2}r^2\left(\frac{1}{-R_{m3}/2+\Delta z}-\frac{1}{R_{m2}/2}\right) \quad (15)$$

The first part of the phase ψ_{opt} is roughly the wave front phase of E_1 in Figure 1, and the second part is the one added by the reflection by RM2, so this phase is roughly the wave front phase of E_{out}. By using Eq.(12) with small $\delta\alpha$ or (14) with $\delta\alpha=0$, the outgoing field E_{out} can be calculated using quantities whose spatial distributions are not affected by the small ROC of focusing cavity mirrors.

4. Propagation using FFT

Eq.(12) gives the expression to calculate the outgoing field, E_{out}, of the FC by using the incoming field, E_{in}. The rapidly oscillating phase ϕ in Eq.(3) and that in Eq. (11), can be suppressed by a proper choice of the scaling factor α. One optimal choice is the one given in Eq.(10), which makes ϕ_{in} to 0 and makes ψ in Eq.(13) suppressed as well.

Because the propagation formula to calculate the outgoing field is a convolution of the incoming field, reflection map with similar spatial structure and the propagation kernel, the size of the FFT grid can be the same as that for the incoming field.

The Fourier transformation of the integral part of Eq. (14) can be written as a product of the Fourier transformation of the product of the incoming field and the reflection map, $\widehat{E}_0$, and that of the propagation kernel with a propagation distance of $(z_1-z_0)/\alpha$, $\widehat{K}$.

$$E_{out}(x_1,y_1,z_1) = C(x_1,y_1,\Delta z,\alpha)\times$$
$$\iint df_x\, df_y \widehat{E_0}(f_x,f_y,z_0)\cdot\widehat{K}(f_x,f_y,\Delta z/\alpha)\cdot\exp(-i2\pi(f_x x_1'+f_y y_1')) \quad (16)$$

The outgoing field is calculated in the following steps.

1) Calculate the source field using Eq.(9).
2) Using the propagation kernel, propagate the source field by $(z_1-z_0)/\alpha$, using the standard FFT.
3) Scale the output coordinate by $1/\alpha$, i.e., switch the coordinate back from (x_1',y_1') to (x_1,y_1).
4) Multiply $C(x_1,y_1,\Delta z,\alpha)$, Eq.(15).

So long as a proper value of α, close to the optimal value, is chosen, the source field, Eq.(9), has similar spatial structure as the incoming field, and no special care is needed when FFT is applied.

5. Practical issues

There are a few practical issues to apply this method. First is the separation of the phase from the mirror reflection map. Mathematically, Eq.(12) can be expressed using M_m, instead of $\overline{M}_m$, together with ϕ_0 in Eq.(7). So long as α is chosen properly, large oscillations in these two functions cancel each other. But, numerically, it often happens that these oscillation phases are calculated in

slightly different ways, and that can introduce imperfect cancellation. So, it is better to use an expression, which excludes any large oscillation explicitly.

Second is the chose of the scaling factor α. The product of two optimal scaling factors, α_{32} for the propagation from RM3 to RM2 and α_{32} for the propagation from RM2 to RM3, is

$$\alpha_{32} \cdot \alpha_{23} = 1 + \frac{4\Delta z^2}{R_{m3} R_{m2}} (1 - \frac{R_{m3} + R_{m2}}{2\Delta z}) \qquad (17)$$

Because $R_{m2}+R_{m3} \neq 2\ \Delta z$, the scaling from RM3 to RM2 and RM2 to RM3 are not reciprocal. But it is close enough that the suppression of the oscillation is enough when one α is chosen to be reciprocal of the other, e.g., α(RM2 to RM3) = 1/ α32.

Usually, the optimal value of α will not give a convenient FFT window size or spacing on one side or both sides of the propagation. It may be convenient to use the optimal value of α for both propagations and apply a smooth interpolation to the FFT grid points, which was set by the user.

6. Numerical results

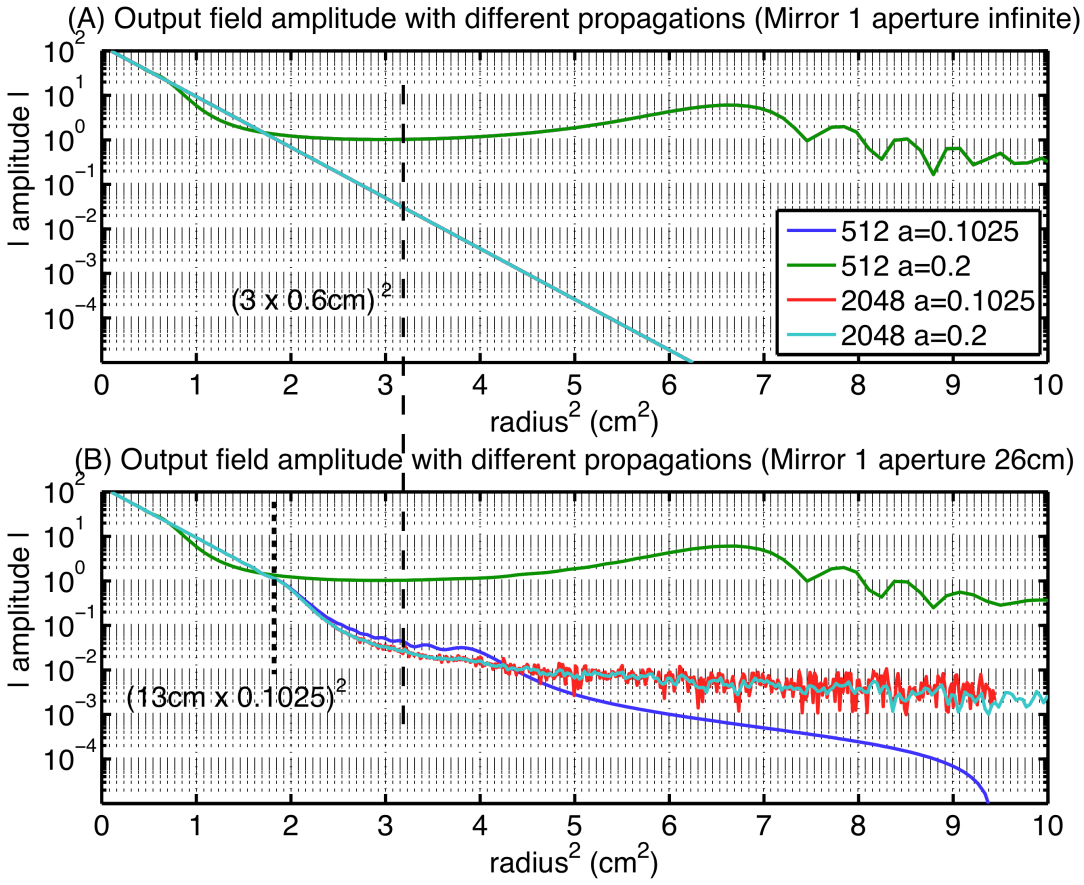

Figure 2 Propagation with different propagation
(In Fig.(A), 3 lines except green overlap each other)

This figure shows amplitudes of the field E_{out} for the same input field, E_{in}, TEM00(ROC=1358m,w=5.4cm), calculated using different propagation methods. Figure (A) is the case when the aperture of RM3 is infinite and (B) is the case when the aperture is 26cm. 512 or 2048 marks the number of FFT grid points. The FFT window size is 60cm on RM3, and the scaling factor α is the optimal value, 0.1025, and an arbitrary value, 0.2.

The beam size on RM2 is 0.6cm, and the 3 times of the beam size is shown by long a dashed line. As is shown in both (A) and (B), when an optimal value is chosen for the scaling factor, the number of grid points can be small (blue), compared to the case using an arbitrary scaling factor (green).

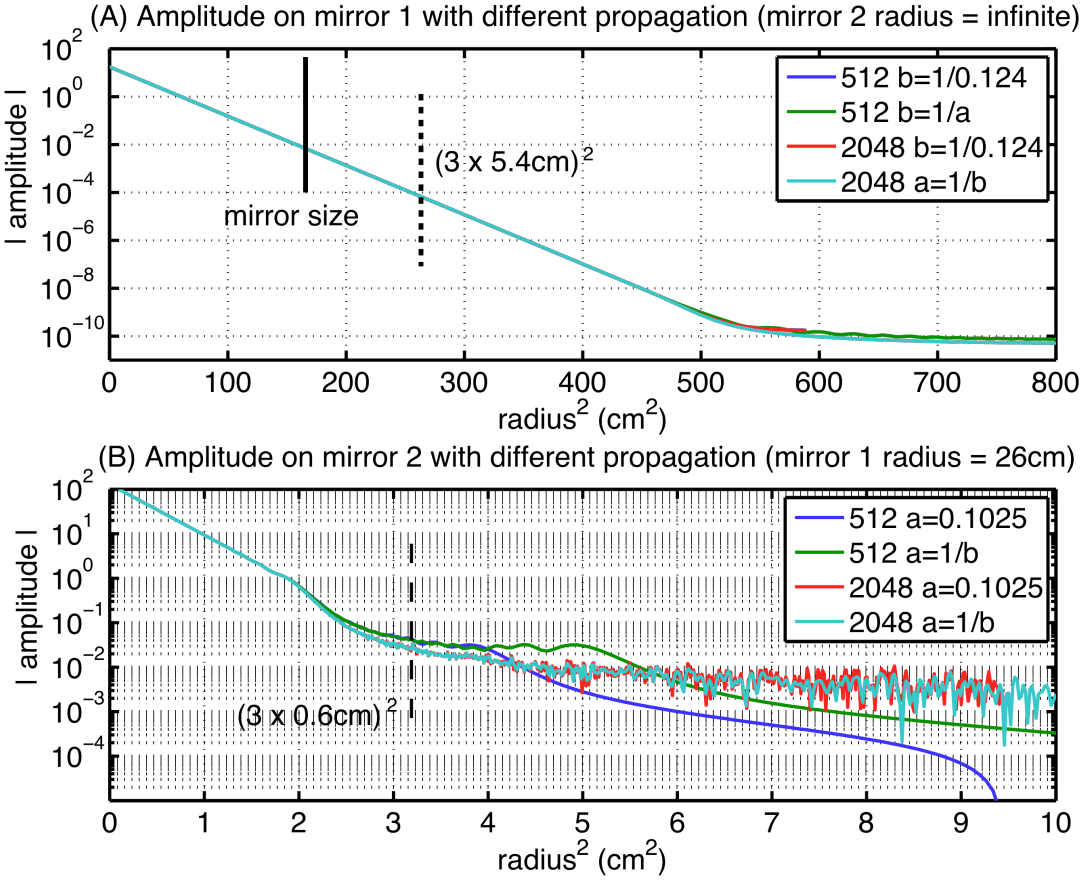

Figure 3 Use of reciprocal values
(For the Fig.(A) calculation, PR3 mirror size is set to infinite to show the tail. The true reflected field will be cut at the line marked as mirror size.)

This figure shows the effect using a reciprocal value of α for one propagation.

Figure (A) is a case for the propagation from RM2 to RM3 (mirror 1 corresponds to RM2 and mirror 2 to RM3). The RM2 aperture is much larger than the beam size. 0.124 is the optimal scaling from RM2 to RM3 and b=1/a means that the scaling factor is calculated using the reciprocal

of the scaling from RM3 to RM2, i.e., 1/0.1025. As is clear that the reciprocal value is close enough that 512 is good enough for the propagation.

Figure (B) is the propagation from RM3 to RM2 (mirror 1 is RM3 and mirror 2 is RM2). The aperture of RM3 is 26cm. Again, up to 3 times of the beam size, marked by long dashed line, 512 is good enough either the optimal value is used (blue) or the reciprocal (green, 1/0.124).

7. Fast simulation in SIS

The algorithm was implemented in SIS [5]. The window sizes of two mirrors are to be specified by the user. For each propagation direction, the phase $\phi_{in}(r)$ in Eq.(9) is evaluated, and if the oscillation at r = 2 w(z) is less than 10, a warning is issued with a suggested range of α.

The alternative method to use α_{opt} as the scaling factor and to smoothly map the result to the user specified window sizes was also tried. This method needs a mapping of distributions of complex field values, and it introduces complex manipulation. The adapted method in SIS to use the scaling factor based on user-specified window sizes does not need tricky manipulations and reasonably window sizes are easily chosen.

The validation of the code was done by calculating fields in a coupled cavity configuration. The apertures of all mirrors are set to be large and all mirror curvatures and the input beam are set to mode match everywhere. Fields simulated by the FFT methods are compared with the modal model calculation and the matching was very good. The higher order mode fractions were order of 1ppm or better at all locations.

8. Effects of finite mirror size

As was shown in the derivation of Eq. (16), the focusing cavity does not introduce any constraint. The true constraint of the number of the FFT grid points, Nfft, comes from the finiteness of mirror apertures and surface aberrations.

Figure 4 and Figure 5 show the profiles of the field in the convergence cavity formed by RM3 and RM2.

The top plots in these figures show the amplitude distribution in the x and y plane. The horizontal axis is x^2 times the sign of x (or y). If the field is a simple gaussian distribution, the plot should be a straight line in both + and – side. The x axis is in the plane of the interferometer and the y axis is vertical to the plane. The beam splitter is rotated around the y axis, so the beam is clipped in the x direction by the finite size of the beam splitter.

Same fields are calculated using Nfft = 512 and 1024. As is shown in the plot, the field can be calculated with good accuracy in the central region. To see the errors in the outer region, the power fraction outside of a circle with a given radius is shown in the lower plot. The radius of RM3 is 13cm, and it is found from this plot the power out of RM3 is 43ppm using Nfft = 1024, while that number is 36 ppm with Nfft = 512.

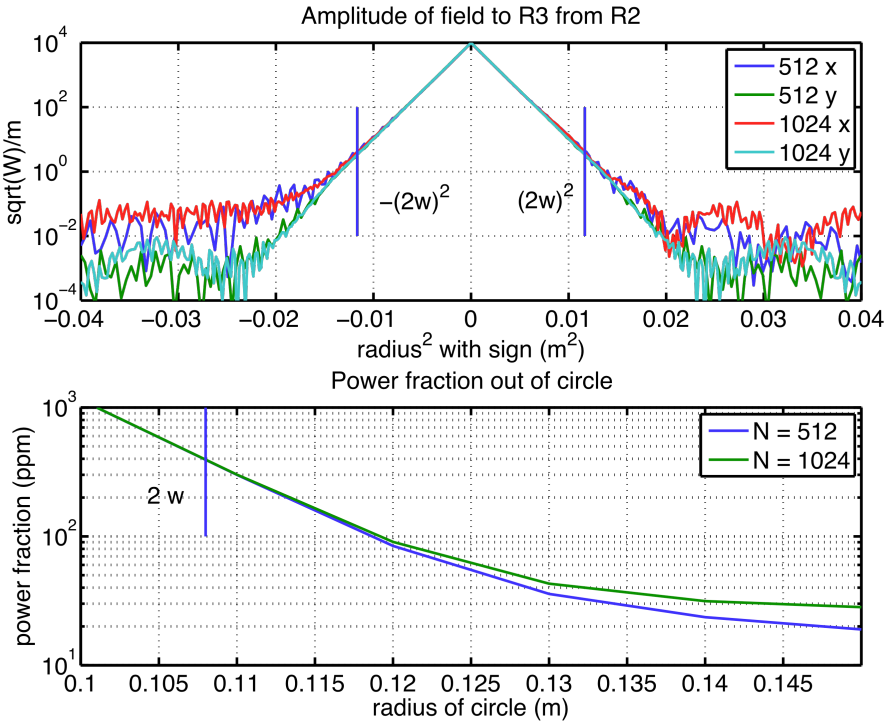

Figure 4 Field to RM3 from RM2

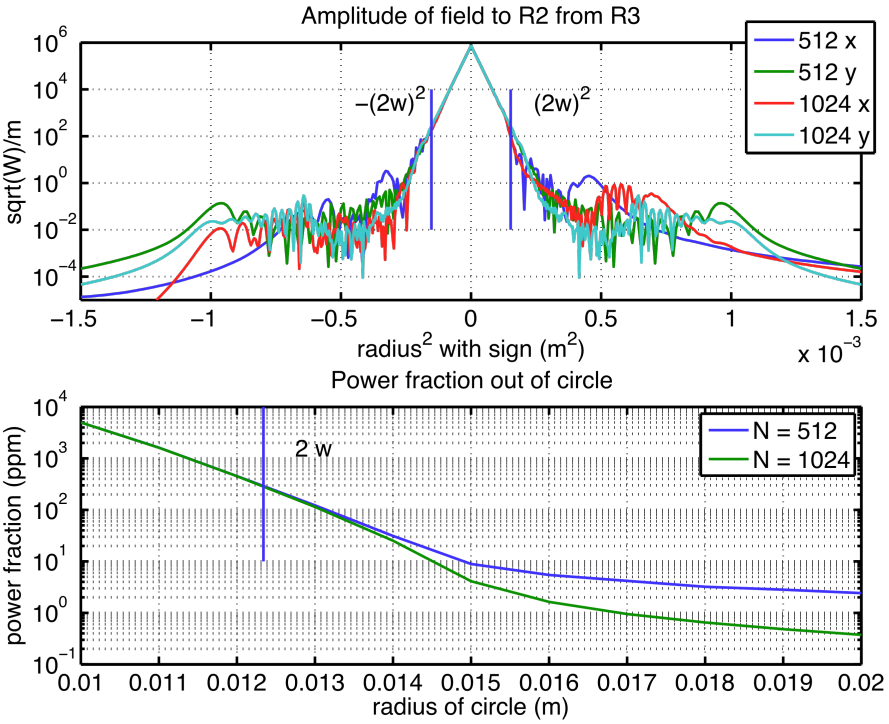

Figure 5 Field to RM2 from RM3

Similar trend is seen from the bottom plot in Figure 5. The radius of RM2 is much larger than the beam size and there is no actual loss due to the finite aperture of RM2. The power stored in the recycling cavity comes out to be 0.0003 larger when calculated using Nfft=512 because of the smaller loss outside of RM3. Because the beam profile in the central region is very well reproduced even when Nfft=512, effects of other imperfections, like fine angle of incidence or the wedge angle will be able to be calculated using small Nfft.

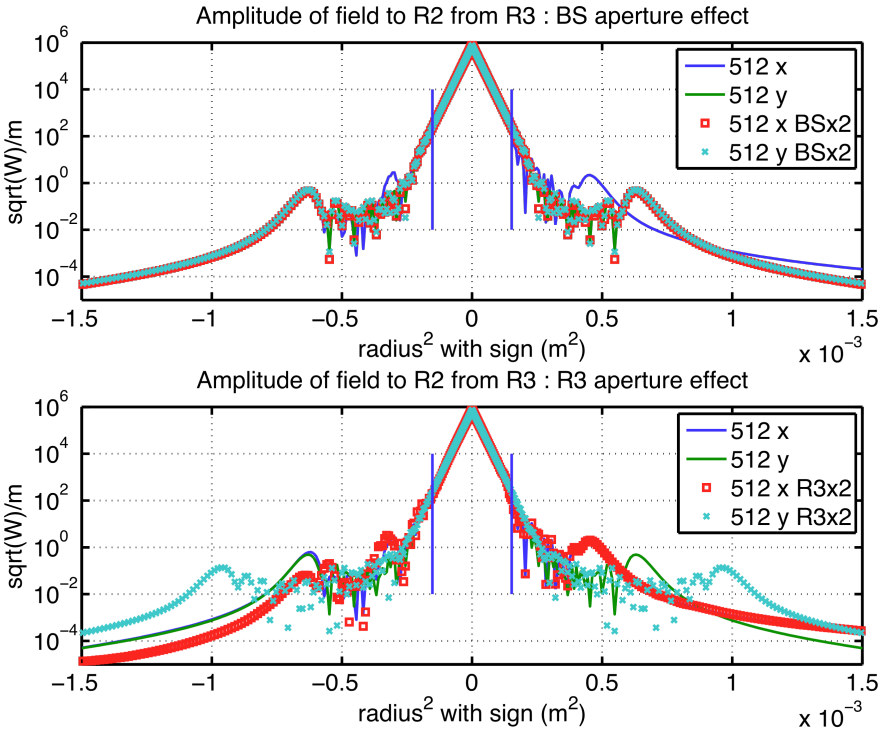

Figure 6 Finite optics effect

Lines with N=512 in the top plot in Figure 5 show structures different from the lines with N=1024. There should not be any dependence on Nfft. To see the cause of these structures, calculations were done with BS aperture doubled (top figure in Figure 6) and with RM3 aperture doubled (bottom plot in the same figure).

The peak at 0.4 10^{-3} (first peak) of the blue line moves to 0.65 10^{-3} when the BS size is doubled, while the two peaks at ±0.65 10^{-3} (second peak) move to ±10^{-3} when the RM3 size is doubled. So the first peak is an ill effect caused by the BS size and the second one by the RM3 size.

9. Summary

When calculating the field propagation through a FC, one needs to properly suppress the spatial oscillation due to the small ROC of the focusing mirrors. The oscillation can be suppressed by choosing a proper scaling of the coordinate on the plane after the propagation. When a proper scaling factor is chosen, the outgoing field after the propagation through the FC can be expressed without explicitly depending on the phase front induced by the reflection of the mirrors forming the FC. So, the FFT parameters to calculate the propagation through the FC is determined

independently of the FC mirror curvatures, i.e., mirror surface aberrations, aperture sizes and parameters of other cavities of the entire interferometer.

10. References

1. P. Fritschel, H. Yamamoto, G. Mueller and M. A. Arain, "Stable Recycling Cavities for Advanced LIGO", LIGO-T080208.
2. M. A. Arain and G. Mueller, "Optical Layout and Parameters for the Advanced LIGO Cavities", LIGO-T0900043.
3. The Virgo collaboration, "The Virgo Physics Book, Vol. II : OPTICS and related TOPICS", April 21, 2006
4. E. A. Sziklas and A. E. Siegman, "Mode calculations in unstable resonators with flowing saturable gain. 2: Fast Fourier transform method", Appl. Opt. 14, 1874-1889 (1975)
5. H. Yamamoto, "SIS (Stationary Interferometer Simulation) manual", LIGO-T070039